THE CORRESPONDENCE BETWEEN STOCHASTIC LINEAR DIFFERENCE AND DIFFERENTIAL EQUATIONS

by D.S.G. POLLOCK
University of Leicester

Modern communications technology relies on the correspondence between continuous signals and discrete sequences sampled from the signals rapidly at regular intervals.

Familiar examples are the analog–digital conversions of digital radio, digital sound recordings and digital television; but the domain of this technology is much wider.

The basis of digital technology is the Shannon–Nyquist sampling theorem, which indicates that, if a signal is sampled with sufficient rapidity, then it can be reconstituted with complete accuracy from the sampled sequence.

The theorem is a commonplace amongst electrical engineers. It ought to be equally familiar to econometricians and statisticians and, in particular, to time-series analysts, but it has been widely ignored.

A common misapprehension regarding a supposed limitation of discrete-time modelling can be illustrated with a quotation from the chapter on *Continuous and Discrete-time Models* that is to be found in the Palgrave volume of *Macroeconometrics and Time Series Analysis*.

A Misunderstanding of the Discrete–Continuous Relationship

There is a common misunderstanding that can be illustrated by quoting a passage from the Palgrave handbook on *Macroeconometrics and Time Series Analysis:*

> "A model built in continuous time can include discrete delays and discontinuities. But, only if all of the delays were discrete multiples of a single underlying time unit and synchronised across agents in the economy, would modelling with a discrete time unit be appropriate."

However, whereas many econometric agents act in an instant under the impact of discrete events, their reactions are rarely precisely synchronised. When the reactions are taken in aggregate, the resulting indices are liable to display slowly evolving low-frequency trajectories, without discontinuities.

Moreover, the analysis overlooks the fundamental theorem that is at the heart of modern digital communications.

The Nyquist–Shannon sampling theorem indicates that, if at least two observations are made in the time that it takes the signal component of highest frequency to complete a single cycle, then a continuous signal can be reconstructed perfectly from the sampled sequence.

The Meaning of the Sampling Theorem

An insight into the relationship between the discrete and the continuous began to emerge in the early years of cinematography.

A moving picture is created from a succession of images that capture instants in the trajectories of moving objects. In the early years of the cinema, the rate at which the images succeeded each other was too slow to produce a convincing depiction of smoothly continuous motion.

An allusion to early cinematography is conveyed by a famous painting by Marcel Duchamp titled *Nude Descending a Staircase,* which was exhibited in 1912 in Paris in the *Salon des Independents.*

When sampling is insufficiently rapid, the sample may be afflicted by the problem of aliasing, whereby high-frequency components of the signal are proxied by motions of lower frequency that fall within the resolution of the sample.

An example of aliasing, which is familiar to cinema goers of more than a certain age, concerns the image of a fleeing stage coach. The rapidly rotating wheels of the coach have a seemingly slow and sometimes retrograde motion.

Sampling at an insufficient rate entails an irremediable loss of information. Sampling at an excessive rate can also lead to problems; but these can be remedied.

A Discrete-time Fourier Analysis.

The Fourier analysis expresses a data sequence $y(t) = \{y_t; t = 0, 1, \ldots, T-1\}$ as

$$y(t) = \sum_{j=0}^{[T/2]} \{\alpha_j \cos(\omega_j t) + \beta_j \sin(\omega_j t)\} = \sum_{j=0}^{T-1} \xi_j e^{-\mathrm{i}\omega_j t}, \tag{1}$$

where $\omega_j = 2\pi j/T; j = 0, \ldots, [T/2]$ are the Fourier frequencies, which are placed at regular intervals running from zero to the Nyquist frequency of π. Here, $[T/2]$ denotes the integer quotient of the division of T by 2.

The coefficients α_j, β_j are obtained by regressing the data on the ordinates of the trigonometric functions $\cos(\omega_j t), \sin(\omega_j t)$, where $t = 0, 1, \ldots, T-1$. Also, $\xi_j = (\alpha_j - \mathrm{i}\beta_j)/2$ and $\xi_{T-j} = (\alpha_j + \mathrm{i}\beta_j)/2$ for $j = 0, 1, \ldots, [T/2]$.

To generate a continuous trajectory that interpolates the data points, one can allow the index t to vary continuously in the interval $[0, T)$. This is described as *Fourier Interpolation*, and the result will be a single cycle of a periodic function.

The periodogram is the plot of the squared amplitudes $\rho_j^2 = \alpha_j^2 + \beta_j^2$, and it conveys a frequency-specific analysis of variance. That is to say

$$V(y) = \frac{1}{T}\sum (y_t - \bar{y})^2 = \frac{1}{2}\sum_j \{\alpha_j^2 + \beta_j^2\} = \frac{1}{2}\sum_j \rho_j^2. \tag{2}$$

Over-rapid Sampling and ARMA Estimation.

If the rate of sampling is in excess of the maximum data frequency, then the periodogram of the data will exhibit a dead space $[\omega_c, \pi]$ running from the the maximum data frequency ω_c up to the limiting Nyquist frequency of π wherein the ordinates $\rho_j^2 = \alpha_j^2 + \beta_j^2$ will have negligible values, attributable only to noise contamination.

The appropriate remedy will be to reconstitute a continuous trajectory by a Fourier synthesis based on the coefficients α_j, β_j from within the frequency interval $[0, \omega_c)$ and to resample the data at the rate of one observation in every time interval of length π/ω_c.

In practice, there may be small elements of noise in the deadspace $[\omega_c, \pi]$, which may have a significant effect when ARMA estimates are obtained from the original data. A quite different effect will arise when the noise is removed from the data.

Figure 1 shows the deviations of the logarithmic quarterly index of real US GDP from a trend determined by the Hodrick–Prescott filter.

Figure 2 shows the periodogram of these data and Figure 3 shows the periodogram of a filtered version of the data from which the deadspace noise has been removed. Figure 4 show the periodogram of the resampled noise-free data.

The parametric spectra of the fitted AR(2) models are superimposed on Figure 2 and 3, whereas the spectrum of an ARMA(2, 1) model is superimposed on Figure 4.

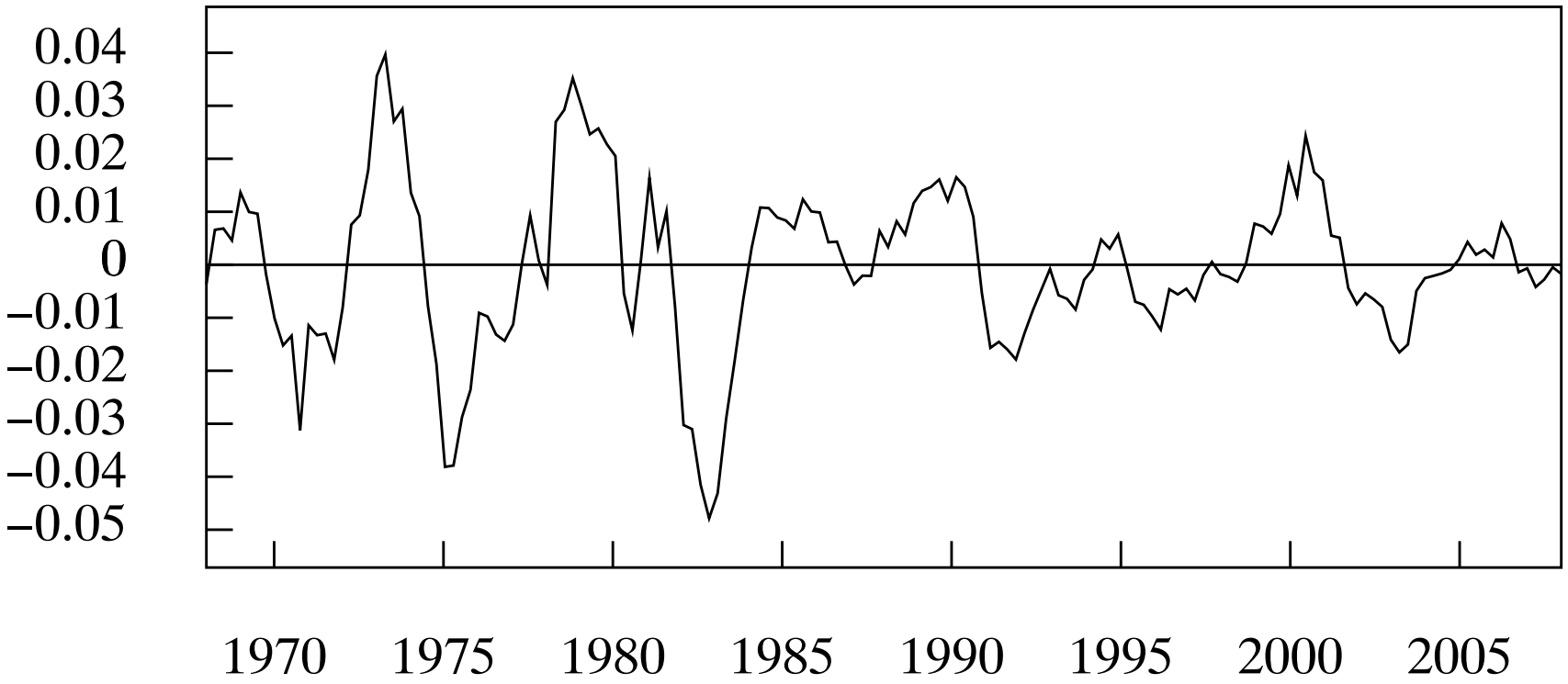

Figure 1. The deviations of the logarithmic quarterly index of real US GDP from an interpolated trend. The observations are from 1968 to 2007. The trend is determined by a Hodrick–Prescott (Leser) filter with a smoothing parameter of 1600.

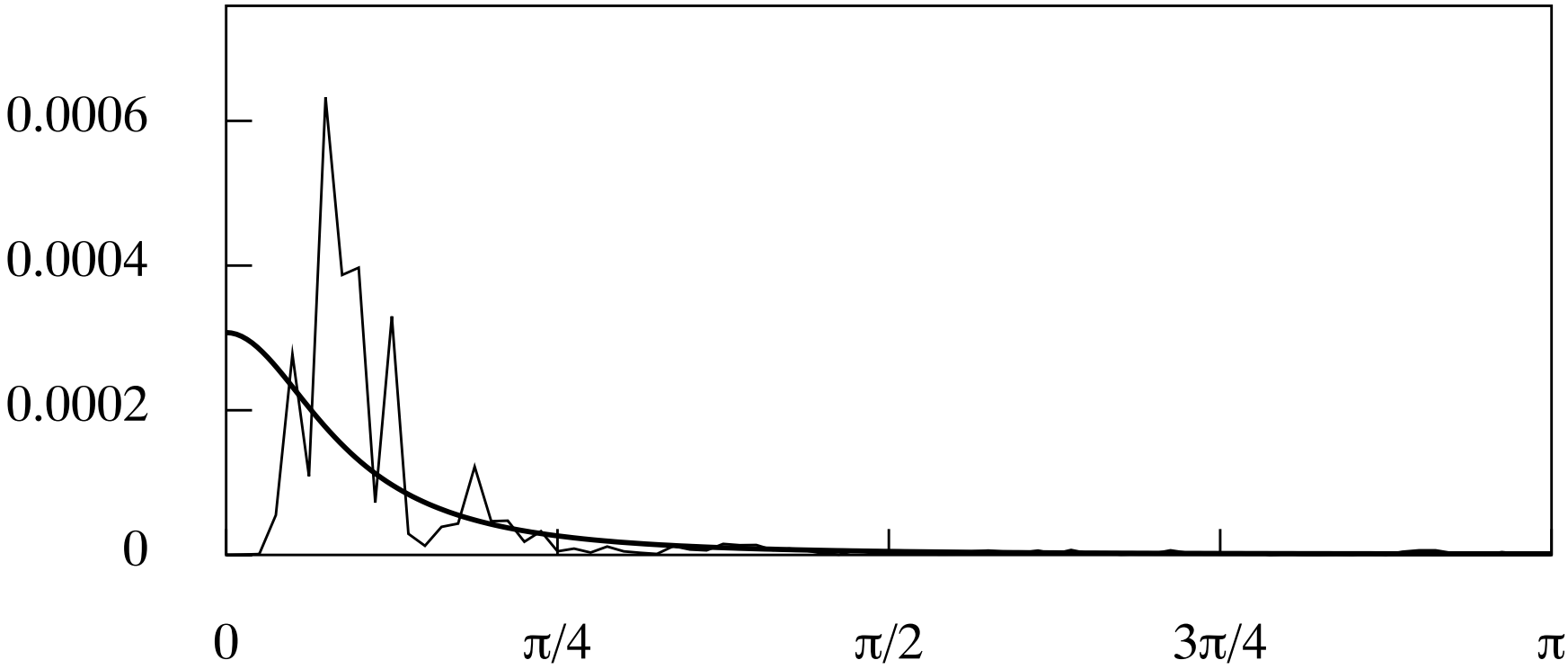

Figure 2. The periodogram of the data points of Figure 1 overlaid by the parametric spectral density function of an estimated regular AR(2) model.

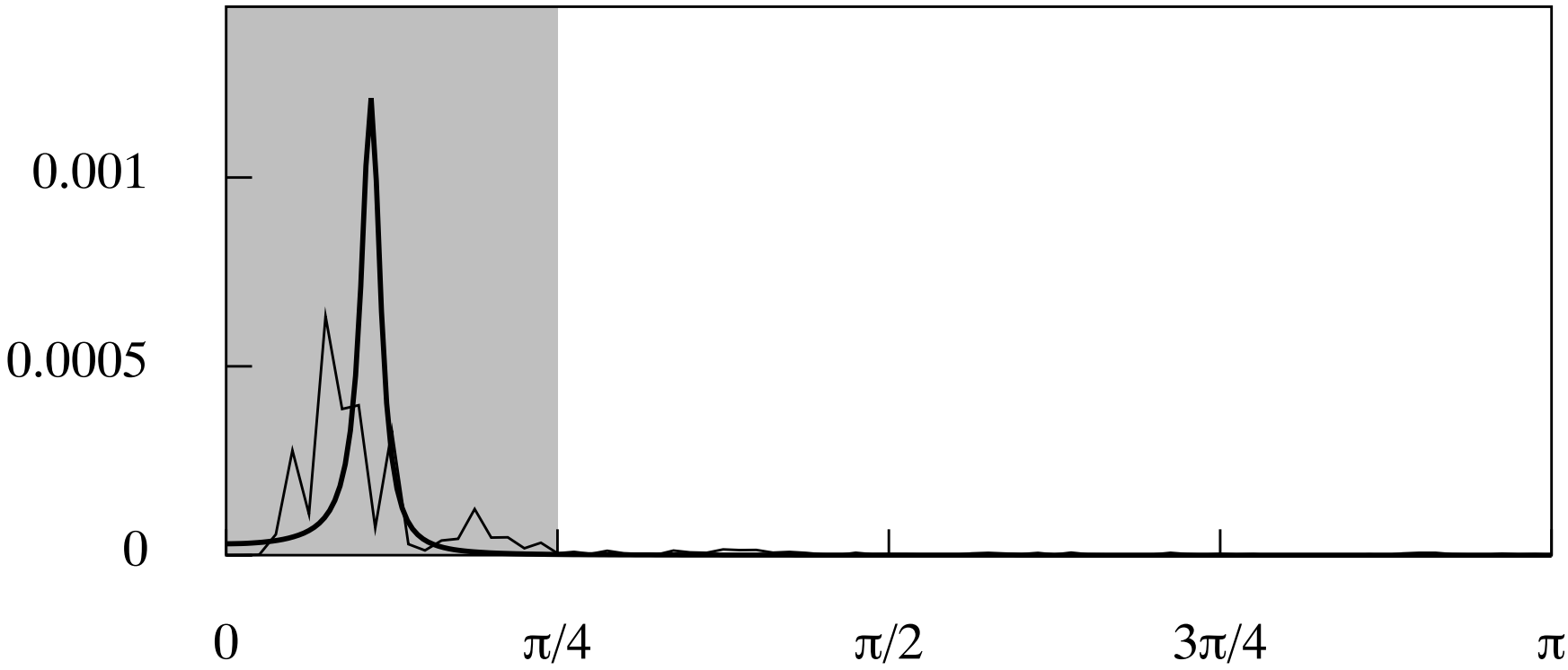

Figure 3. The periodogram of the data points of Figure 1 overlaid by the spectral density function of an AR(2) model estimated from frequency-limited data.

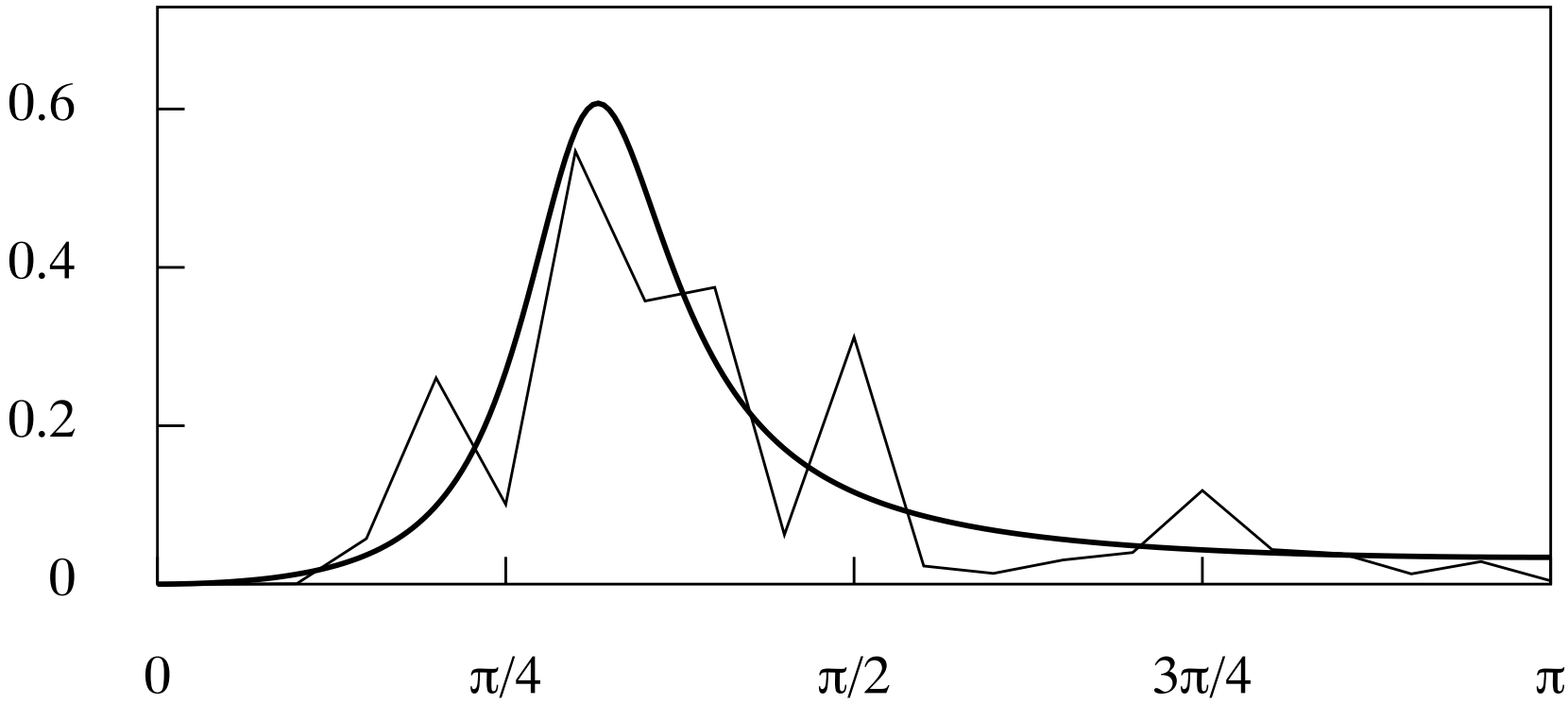

Figure 4. The periodogram of the data that have been filtered and subsampled at the rate of 1 observation in 4, overlaid by the parametric spectrum of an estimated ARMA(2, 1) model.

Explaining the Results of the ARMA Estimations.

When there is noise contamination

The noise makes a significant contribution to the variance of the data without affecting the autocovariances at positive lags. As a result, the initial values, which determine the estimates of the autoregressive parameters, will show an exaggerated rate of decline, which will give rise to real-valued roots.

In the absence of noise contamination

When the rate of sampling is excessive, the autocovariances will be sampled at points that are too close to the origin, where the variance is to be found. Then, their values will decline at a diminished rate. The reduction in the rate of convergence will be reflected in the modulus of the estimated complex roots, which will understate the rate of damping.

De-noising and resampling the data

Although the white-noise contamination extends uniformly over the interval $[0, \pi]$, it is sufficient to remove it from the interval $[\omega_c, \pi]$ by setting the corresponding Fourier coefficients to zero. Having created a continuous data trajectory by a Fourier synthesis based on the coefficients in the interval $[0, \omega_c]$, the data are resampled at intervals of π/ω_c time units. The periodogram of the resampled data will extend over the entire Nyquist interval $[0, \pi]$, which is appropriate to an ARMA model.

The Frequency-Limited Continuous-time ARMA model.

A continuous-time model can be derived readily from a discrete-time ARMA model that has been fitted to the data. This is achieved by attaching appropriately scaled sinc function kernels to each of the impulses of the discrete model and by summing the superimposed ordinates.

A sinc function centered on k is defined by

$$\varphi(t-k) = \frac{1}{2\pi}\int_{-\pi}^{\pi} e^{\mathrm{i}\omega(t-k)}d\omega = \frac{\sin\{\pi(t-k)\}}{\pi(t-k)}. \tag{3}$$

Within the discrete-time ARMA equation

$$\sum_{i=0}^{p}\alpha_i y_{t-i} = \sum_{i=0}^{q}\beta_i\varepsilon_{t-i} \tag{4}$$

a sinc function is associated to each element, implying the following replacements:

$$y_t \longrightarrow y(t) = \sum_{k=-\infty}^{\infty} y_{t-k}\varphi(t-k) \quad \text{and} \quad \varepsilon_t \longrightarrow \varepsilon(t) = \sum_{k=-\infty}^{\infty} \varepsilon_{t-k}\varphi(t-k). \tag{5}$$

The equivalence of the discrete and continuous processes in indicated by the Nyquist–Shannon sampling theorem.

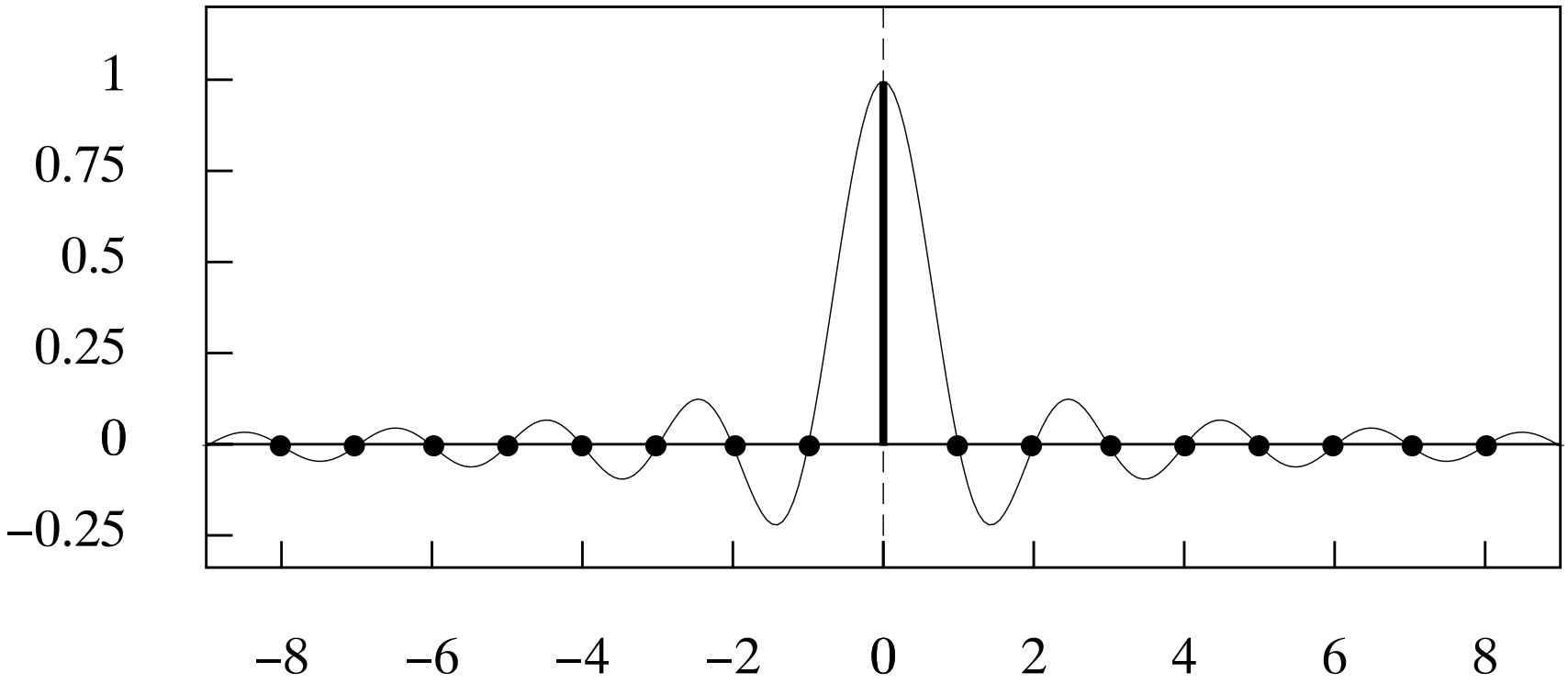

Figure 5. The sinc function wave-packet $\varphi(t) = \sin(\pi t)/\pi t$ comprising frequencies in the interval $[0, \pi]$.

The Nyquist-Shannon Sampling Theorem

The Fourier integral transform has the following expressions in the time domain and the frequency domain:

$$x(t) = \frac{1}{2\pi}\int_{-\infty}^{\infty} \xi(\omega)e^{\mathrm{i}\omega t}d\omega \longleftrightarrow \xi(\omega) = \int_{-\infty}^{\infty} x(t)e^{-\mathrm{i}\omega t}dt. \tag{6}$$

However, with the frequencies bounded by the Nyquist value of π, this becomes

$$x(t) = \frac{1}{2\pi}\int_{-\pi}^{\pi} \xi_S(\omega)e^{\mathrm{i}\omega t}d\omega \longleftrightarrow \xi_S(\omega) = \sum_{k=-\infty}^{\infty} x_k e^{-\mathrm{i}k\omega}, \tag{7}$$

where $\{x_k; k = 0, \pm 1, \pm 2, \ldots\}$ is sampled at unit intervals from $x(t)$. Putting the RHS of (7) into the LHS and interchanging the order of integration and summation gives

$$x(t) = \frac{1}{2\pi}\sum_{k=-\infty}^{\infty} x_k \left\{\int_{-\pi}^{\pi} e^{\mathrm{i}\omega(t-k)}\right\} d\omega = \sum_{k=-\infty}^{\infty} x_k \varphi(t-k), \tag{8}$$

where

$$\varphi(t-k) = \frac{\sin\{\pi(t-k)\}}{\pi(t-k)} \tag{9}$$

is a the so-call sinc function. The RHS of equation (8) defines a sinc function interpolation.

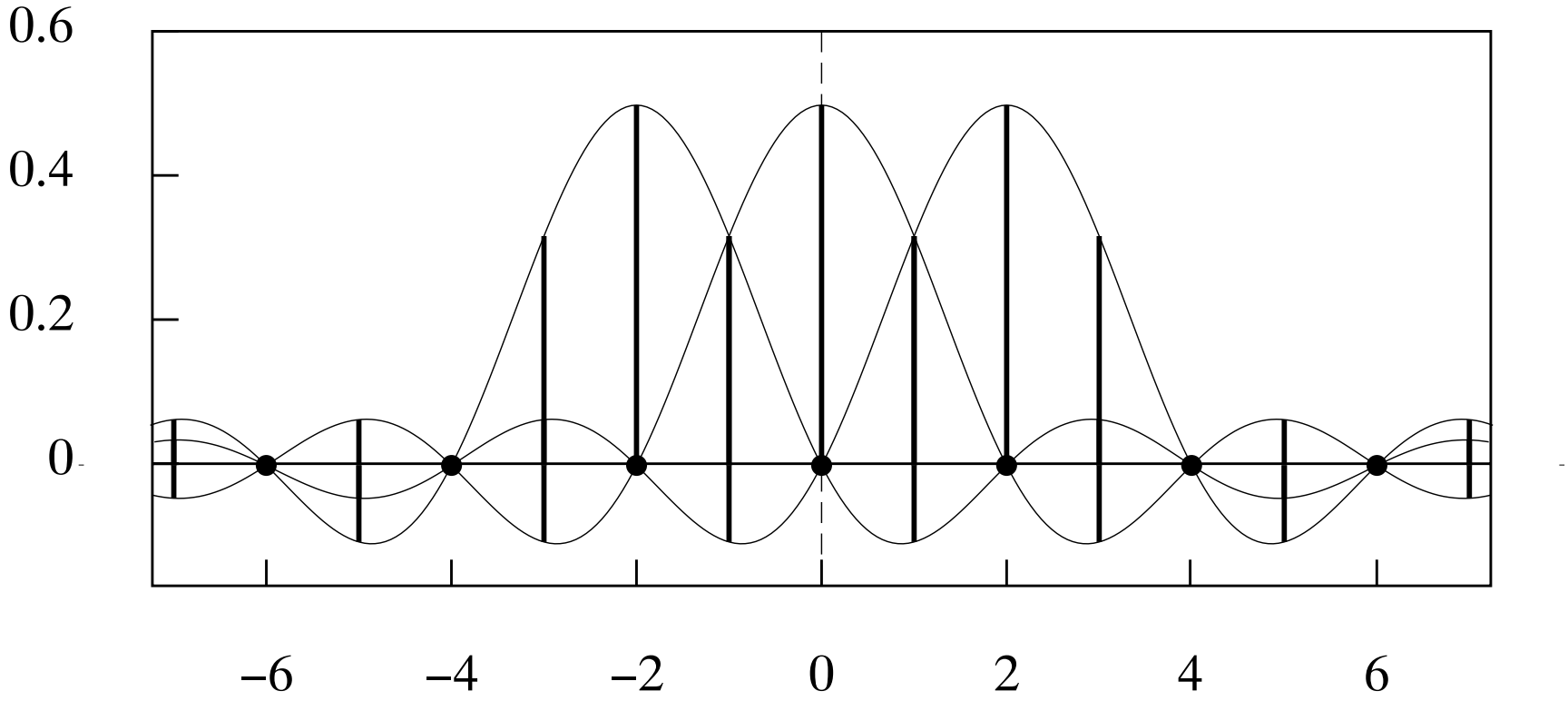

Figure 6. The wave packets $\varphi(t/2 - k)$, which are bounded in frequency by $\pi/2$, suffer no mutual interference when $k \in \{0, \pm 2, \pm 4, \pm 6, \ldots\}$.

The Wrapped Sinc Function and the Dirichlet Kernel

An evident difficulty with this theorem lies in the fact that the sinc functions are supported on the entire real line.

Therefore, every sinc function that is indexed by the integers $\{k = 0, \pm 1 \pm 2, \ldots\}$, denoting their displacements, will be present at every point on the real line.

This means that the process of creating the continuous trajectory by adding the sinc functions of varying amplitudes and at successive displacements would entail an infinite sum.

However, the empirical data sequences, which are supported only on a finite set of T contiguous integer points, can be regarded as circular sequences. Therefore, the kernel functions that are to be applied to the sampled ordinates are circular or, equivalently, periodic sinc functions.

The sinc functions are wrapped around the circle of circumference T and their overlying ordinates are added to create so-called Dirichlet kernels. These kernels are applied to the circular data sequence in place of the sinc functions.

The set of Dirichlet kernels at unit displacements provides the basis for the set of periodic functions limited in frequency to the Nyquist interval $[-\pi, \pi]$.

The Wrapped Sinc Function and the Dirichlet Kernel

Let ξ_j^S be the jth ordinate from the discrete Fourier transform of $T = 2n$ points sampled from the function. If the function is frequency-limited to π radians, then there is

$$x(t) = \sum_{j=0}^{T-1} \xi_j^S e^{\mathrm{i}\omega_j t} \longleftrightarrow \xi_j^S = \frac{1}{T} \sum_{t=0}^{T-1} x_t e^{-\mathrm{i}\omega_j t}, \qquad \omega_j = \frac{2\pi j}{T}. \tag{10}$$

Putting the expression for the Fourier ordinates into the series expansion of the time-domain function and commuting the summation signs gives

$$x(t) = \sum_{j=0}^{T-1} \left\{ \frac{1}{T} \sum_{k=0}^{T-1} x_k e^{\mathrm{i}\omega_j k} \right\} e^{\mathrm{i}\omega_j t} = \frac{1}{T} \sum_{k=0}^{T-1} x_k \left\{ \sum_{j=0}^{T-1} e^{\mathrm{i}\omega_j (t-k)} \right\}. \tag{11}$$

The inner summation gives rise to the Dirichlet kernel:

$$\varphi_n^\circ(t) = \sum_{t=0}^{T-1} e^{\mathrm{i}\omega_j t} = \frac{\sin([n-1/2]\omega_1 t)}{\sin(\omega_1 t/2)}, \qquad \omega_1 = \frac{2\pi}{T}. \tag{12}$$

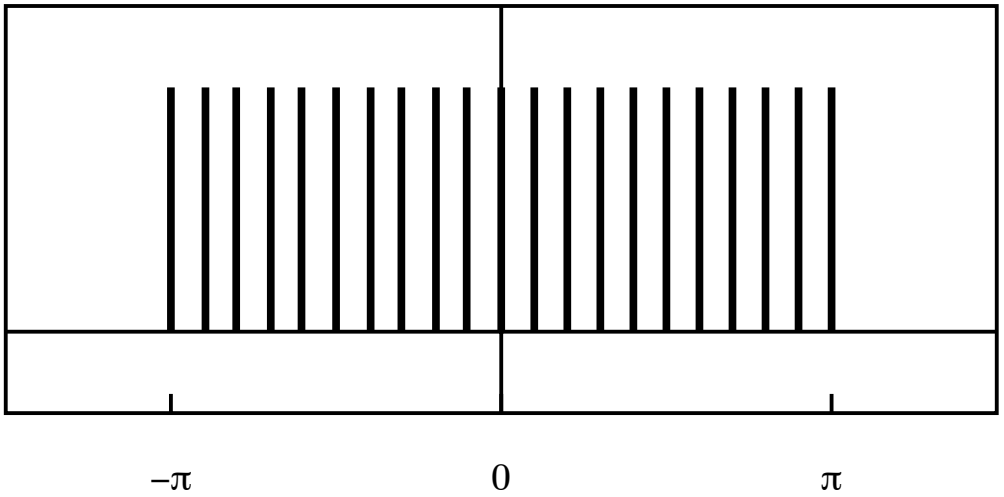

Figure 7. The frequency-domain rectangle sampled at $M = 21$ points.

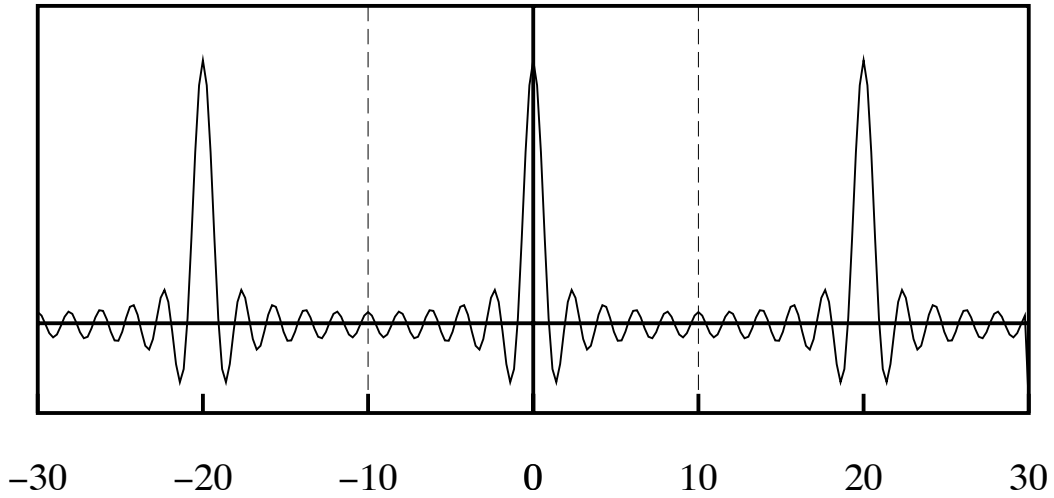

Figure 8. The Dirichlet function $\sin(\pi t)/\sin(\pi t/M)$ obtained from inverse Fourier transform of a frequency-domain rectangle sampled at $M = 21$ points.

Fourier Interpolation and Dirichlet Kernel Interpolation

What this shows is that the Fourier expansion can be expressed in terms of the Dirichlet kernel, which is a circularly wrapped sinc function:

$$x(t) = \frac{1}{T}\sum_{k=0}^{T-1} x_k \varphi_n^\circ(t-k), \quad \text{where} \quad \varphi_n^\circ(-k) = \varphi_n^\circ(T-k). \tag{13}$$

The functions $\{\varphi^\circ(t-k); k = 0, 1, \ldots, T-1\}$ are appropriate for reconstituting a continuous periodic function $x(t)$ defined on the interval $[0, T)$ from its sampled ordinates $x_0, x_1, \ldots, x_{T-1}$.

However, the periodic function can also be reconstituted by an ordinary Fourier interpolation

$$x(t) = \sum_{j=0}^{T-1} \xi_j e^{\mathrm{i}\omega_j t} = \sum_{j=0}^{[T/2]} \left\{\alpha_j \cos(\omega_j t) + \beta_j \sin(\omega_j t)\right\}, \tag{14}$$

where $[T/2]$ denotes the integral part of $T/2$ and where $\alpha_j = \xi_j + \xi_{T-j}$ and $\beta_j = \mathrm{i}(\xi_j - \xi_{T-j})$ are the coefficients from the regression of the data on the sampled ordinates of the cosine and sine functions at the various Fourier frequencies.

Linear Stochastic Differential Equations

There is also a linear stochastic differential equation (LSDE) that corresponds to the difference equation of the ARMA model.

The first-order autoregressive equation takes the form of

$$y(t) = \mu y(t-1) + \varepsilon(t) \qquad \text{or} \qquad y(t) = \frac{\varepsilon(t)}{1-\mu L} = \sum_{\tau=0}^{\infty} \mu^{\tau} \varepsilon(t-\tau). \tag{15}$$

The corresponding first-order stochastic differential equation is denoted by

$$\frac{dy}{dt} = \kappa y(t) + \zeta(t) \qquad \text{or} \qquad y(t) = \frac{\zeta(t)}{D-k} = \int_0^{\infty} e^{\kappa\tau} \zeta(t-\tau). \tag{16}$$

The integral on the interval $(-\infty, t]$ may be separated into two parts, which are the intervals over $(-\infty, t-1]$ and $(t-1, t]$:

$$\begin{aligned} y(t) &= e^{\kappa} \int_{-\infty}^{t-1} e^{\kappa(t-1-\tau)} \zeta(\tau) d\tau + \int_{t-1}^{t} e^{\kappa(t-\tau)} \zeta(\tau) d\tau \\ &= \mu y(t-1) + \varepsilon(t). \end{aligned} \tag{17}$$

Discrete and Continuous Models of Higher Orders

In the absence of repeated poles, the ARMA(p, q) model has the following partial-fraction representation:

$$\begin{aligned} y(t) = \frac{\beta(L)}{\alpha(L)}\varepsilon(t) &= \frac{\beta_0 + \beta_1 L + \cdots + \beta_q L^q}{1 + \alpha_1 L + \cdots + \alpha_p L^p}\varepsilon(t) \\ &= \left\{ \frac{d_1}{1 - \mu_1 L} + \frac{d_2}{1 - \mu_2 L} + \cdots + \frac{d_p}{1 - \mu_p L} \right\} \varepsilon(t) \\ &= \sum_{\tau=0}^{\infty} \left\{ d_1 \mu_1^\tau + d_2 \mu_2^\tau + \cdots + d_p \mu_2^\tau \right\} \varepsilon(t - \tau). \end{aligned} \tag{18}$$

Likewise, the LSDE(p, q) can be represented by

$$\begin{aligned} y(t) = \frac{\theta(D)}{\phi(D)}\zeta(t) &= \frac{\theta_0 D^q + \theta_1 D^{q-1} + \cdots + \theta_q}{\phi_0 D^p + \phi_1 D^{p-1} + \cdots + \phi_p}\zeta(t) \\ &= \left\{ \frac{c_1}{D - \kappa_1} + \frac{c_2}{D - \kappa_2} + \cdots + \frac{c_p}{D - \kappa_p} \right\} \zeta(t) \\ &= \int_0^{\infty} \left\{ c_1 e^{\kappa_1 \tau} + c_2 e^{\kappa_2 \tau} + \cdots + c_p e^{\kappa_p \tau} \right\} \zeta(t - \tau) d\tau. \end{aligned} \tag{19}$$

Discrete and Continuous Frequency-limited Models

A correspondence can be established between the discrete and continuous systems by invoking the principle of *impulse invariance.*

This indicates that a sequence sampled at unit intervals from the impulse response function of the continuous system should be equal to the impulse response of the discrete-time system.

This is only possible if the continuous system has the same frequency limitation as the discrete system, which is the present assumption.

Thus, at the integer values of τ, the impulse response functions

$$\psi(t) = c_1 e^{\kappa_1 \tau} + c_2 e^{\kappa_2 \tau} + \cdots + c_p e^{\kappa_p \tau} \tag{20}$$

and

$$\phi(\tau) = d_1 \mu_1^\tau + d_2 \mu_2^\tau + \cdots + d_p \mu_2^\tau \tag{21}$$

should be equal. The equality can be achieved by setting $e^{\kappa_j} = \mu_j$ and $c_j = d_j$, for all j.

Mapping from an ARMA Model to a Continuous-time CARMA model

To illustrate the mapping from an ARMA model to a continuous frequency-limited CARMA model, an ARMA(2, 1) model is chosen with conjugate complex poles $\alpha \pm \mathrm{i}\beta = \rho \exp\{\pm \mathrm{i}\theta\}$, where $\rho = \sqrt{\alpha^2 + \beta^2} = 0.9$ and $\theta = \tan^{-1}(\beta/\alpha) = \pi/4 = 45°$. The moving-average component has a zero of 0.5. The ARMA process generates prominent cycles of an average duration of roughly 8 periods.

Figure 8 shows the spectrum of the ARMA process. Since the function is virtually zero at the limiting frequency of π, it is reasonable to propose a corresponding continuous-time model driven by a white-noise forcing function that is bounded by the Nyquist frequency.

The principle of *impulse invariance* is used in finding the parameters of the continuous-time CARMA model, which are displayed beside those of the corresponding ARMA model:

ARMA	CARMA
$\alpha_0 = 1.0$	$\phi_0 = 1.0$
$\alpha_1 = -1.2728$	$\phi_1 = 0.2107$
$\alpha_2 = 0.8100$	$\phi_2 = 0.6280$
$\beta_0 = 1.0$	$\theta_0 = 1.0$
$\beta_1 = -0.5$	$\theta_1 = 0.2737$

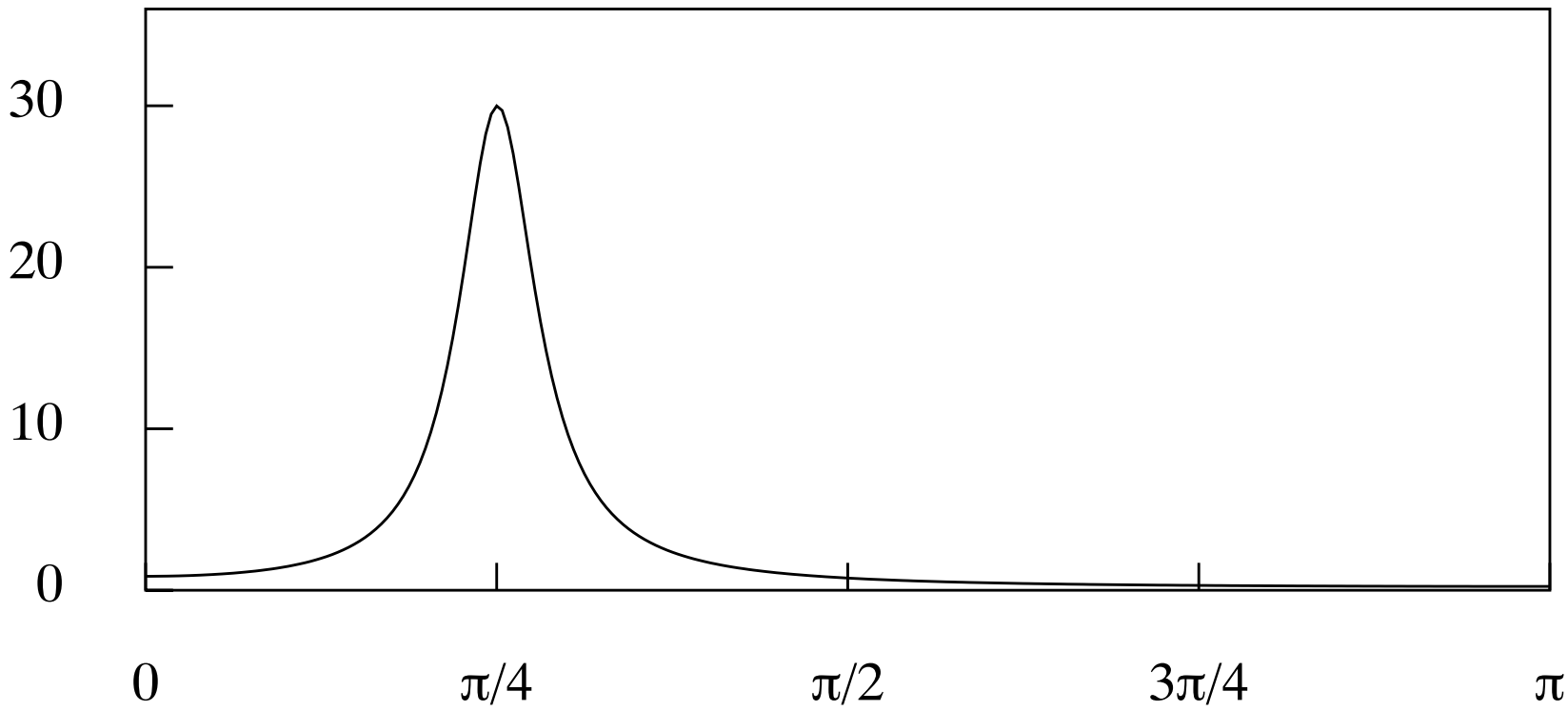

Figure 9. The spectrum of the ARMA(2, 1) process $(1.0 - 1.273L + 0.81L^2)y(t) = (1 - 0.5L)e(t)$.

The Autocovariance Functions

The general analytic expression for the autocovariance function of an ARMA process is

$$\gamma^d(\tau) = \sigma_\varepsilon^2 \sum_{i=1}^{p} \Big\{ \sum_{j=1}^{p} \frac{d_i d_j}{1 - \mu_i \mu_j} \Big\} \mu_i^\tau . \tag{22}$$

Based on the transfer function $\psi(t) = \sum c_i e^{\kappa_i t}$, the autocovariance generating function of the LSDE process driven by a Wiener process is

$$\begin{aligned} \gamma^c(\tau) = \sigma_\zeta^2 \int_0^\infty \psi(t)\psi(t+\tau)dt &= \sigma_\zeta^2 \sum_{i=1}^{p} \sum_{j=1}^{p} \Big\{ c_i c_j \int_0^\infty e^{(\kappa_i+\kappa_j)t+\kappa_i\tau} dt \Big\} \\ &= \sigma_\zeta^2 \sum_{i=1}^{p} \Big\{ \sum_{j=1}^{p} c_i c_j \frac{-e^{\kappa_i \tau}}{\kappa_i + \kappa_j} \Big\}. \end{aligned} \tag{23}$$

The mappings between the discrete and the continuous models are obtained by equating the corresponding autocovariance functions at the sampling intervals.

If μ is a complex root of the discrete process and κ is a corresponding root of the continuous process, then the mapping $\mu \longrightarrow \kappa$ is one to many:

$$\mu = e^\kappa = e^\delta \{\cos(\omega + 2\pi n) + \mathrm{i} \sin(\omega + 2\pi n)\}. \tag{24}$$

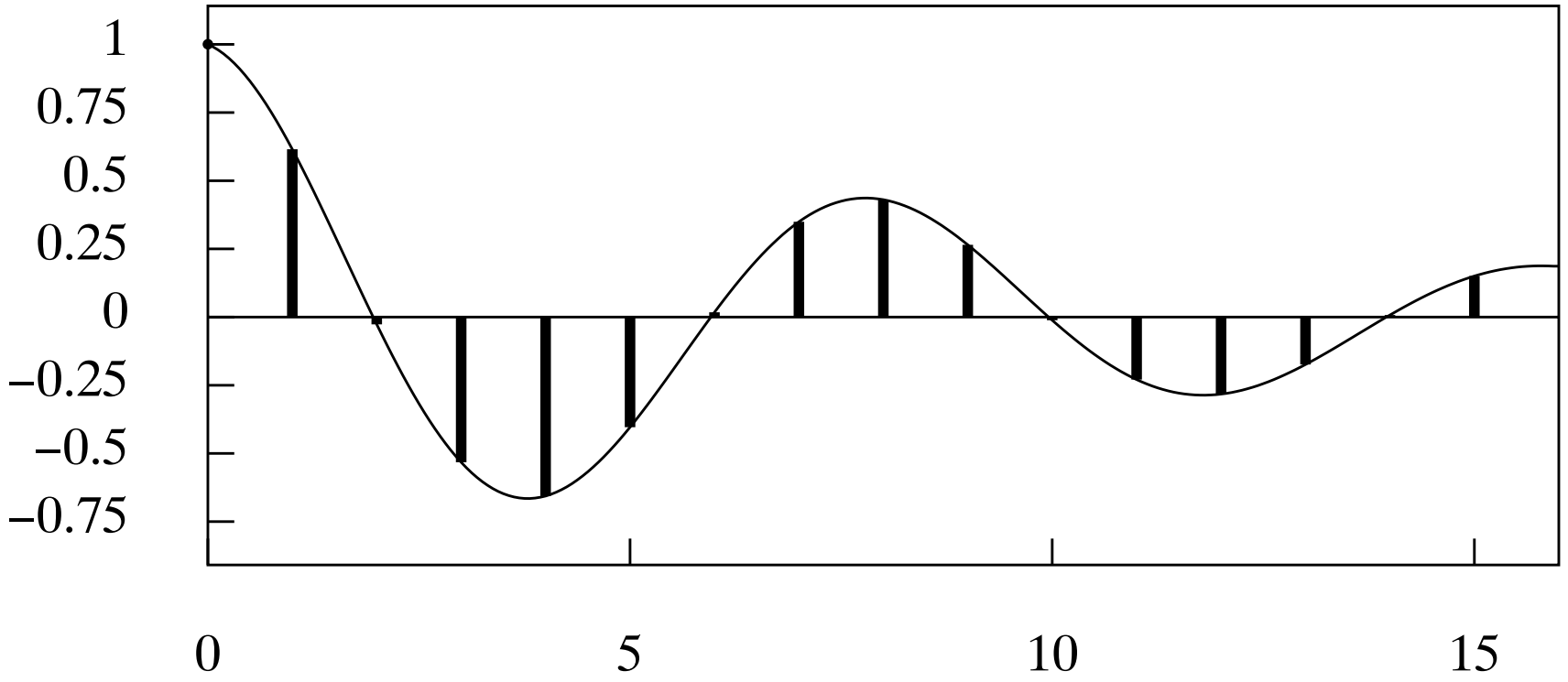

Figure 10. The discrete autocovariance sequence of the ARMA(2, 1) process and the continuous autocovariance function of the corresponding CARMA(2, 1) process.

Spectral Density Functions

The autocovariance generating function of the ARMA process is

$$\gamma^d(z) = \sigma_\varepsilon^2 \frac{\beta(z)\beta(z^{-1})}{\alpha(z)\alpha(z^{-1})} = \sigma_\varepsilon^2 \psi(z)\psi(z^{-1}). \tag{25}$$

Running ω over the interval $[-\pi, \pi]$, generates a periodic spectral density function, which is the discrete-time Fourier transform of the sequence of autocovariances:

$$f^d(\omega) = \frac{1}{2\pi} \sum_{\tau=-\infty}^{\infty} \gamma_\tau^d e^{-\mathrm{i}\omega\tau} = \frac{1}{2\pi}\Big\{\gamma_0^d + 2\sum_{\tau=1}^{\infty} \gamma_\tau^d \cos(\omega\tau)\Big\}. \tag{26}$$

The spectral density function $f^c(\omega)$ of the continuous-time process is the Fourier integral transform of autocovariance function:

$$f^c(\omega) = \frac{1}{2\pi} \int_{-\infty}^{\infty} \gamma^c(\tau) e^{-\mathrm{i}\omega\tau} d\tau = \frac{1}{\pi} \int_0^{\infty} \gamma^c(\tau) \cos(\omega\tau) d\tau. \tag{27}$$

This is not a periodic function. In the case of an LSDE(p, q) there is

$$f^c(\omega) = \frac{\sigma_\zeta^2}{2\pi} \frac{|\theta_0(\mathrm{i}\omega)^p + \theta_1(\mathrm{i}\omega)^{p-1} + \cdots + \theta_q|^2}{|(\mathrm{i}\omega)^p + \phi_1(\mathrm{i}\omega)^{p-1} + \cdots + \phi_p|^2}. \tag{28}$$

Estimation of the Unlimited LSDE by the Autocovariance Principle

If a complex pole of the ARMA model takes the form of

$$\mu = \alpha + \mathrm{i}\beta = \rho e^{\mathrm{i}\omega} \quad \text{with} \quad \rho = \sqrt{\alpha^2 + \beta^2} \quad \text{and} \quad \omega = \tan^{-1}\left(\frac{\beta}{\alpha}\right), \tag{29}$$

then the corresponding pole of the LSDE and of the CARMA differential equation is

$$\kappa = \ln(\mu) = \ln(\rho) + \mathrm{i}\omega = \delta + \mathrm{i}\omega, \tag{30}$$

with $\delta \in (-\infty, 0)$, which puts it in the left half of the s-plane.

The principle of *autocovariance equivalence* can be expressed via the equation

$$\gamma_\tau^c\{\kappa(\mu), c\} = \gamma_\tau^d(\mu, d), \quad \text{for} \quad \tau \in \{0, \pm 1, \pm 2, \ldots\}. \tag{31}$$

The LSDE parqameters can be derived once a value of $c = [c_1, c_2, \ldots, c_p]$ of the numerator coefficients of the partial fraction expansion has been found that satisfies this equation.

The value of c can be found by using the Nelder–Mead optimisation procedure to find the zeros of

$$z(c) = \sum_{\tau=0}^{p} \{\gamma_\tau^c(c) - \gamma_\tau^d\}^2. \tag{32}$$

Mapping from an ARMA Model to an Unrestricted LSDE model

The previously specified ARMA(2, 1) model can be mapped to a continuous-time LSDE model via the principle of *autocovariance equivalence*. Although the forcing function of the LSDE is unbounded in frequency, the transfer function imposes a strong attenuation on the higher frequencies that implies a virtual frequency limitation.

The spectral density function of the LSDE model virtually coincides with that of the ARMA and of the CARMA model over the interval $[0, \pi]$. Also, the autocovariance functions are virtually identical.

However, whereas the autoregressive parameters are identical, there is an unexpected disparity between the moving-average parameters of the CARMA and the LSDE, albeit that the ARMA parameters can be recovered exactly from those of the LSDE.

CARMA	LSDE
$\phi_0 = 1.0$	$\phi_0 = 1.0$
$\phi_1 = 0.2107$	$\phi_1 = 0.2107$
$\phi_2 = 0.6280$	$\phi_2 = 0.6280$
$\theta_0 = 1.0$	$\theta_0 = 0.9088$
$\theta_1 = 0.2737$	$\theta_1 = 0.5601$

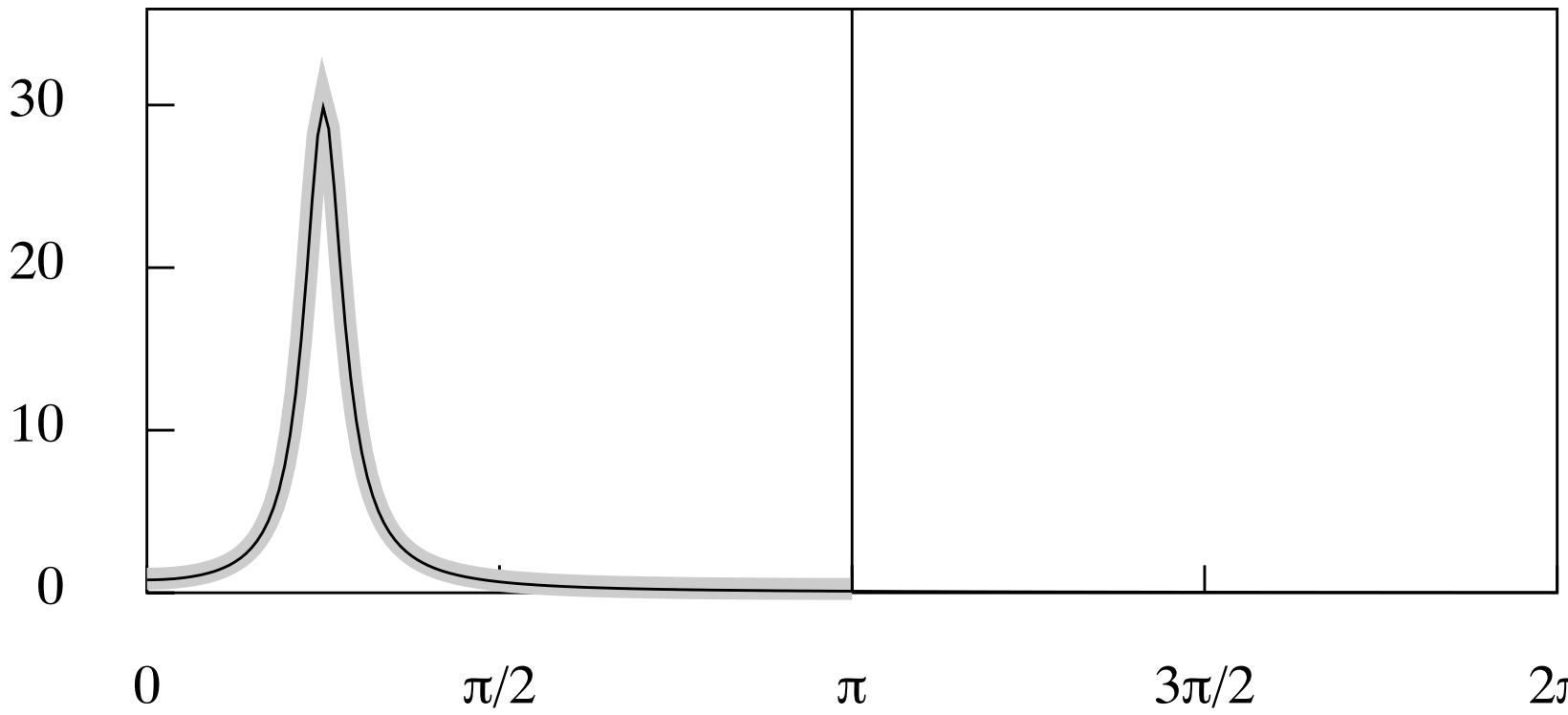

Figure 11. The spectrum of the LSDE(2, 1) corresponding to the ARMA(2, 1) model of Example 1 plotted on top of the spectrum of that model, represented by the thick grey line. The two spectra virtually coincide over the interval $[0, \pi]$.

The Contours of the Criterion Function

The divergence of the moving-average parameters may be investigated via the contour map of the function $z(a, b)$, which is the sum of squares of the differences of the autocovariance functions of the ARMA and LSDE models at the integer points. The parameters a, b are from the numerator coefficients $c, c^* = a \pm \mathrm{i}b$ of the partial-fraction decomposition of the LSDE(2, 1) transfer function.

The contour map on the LHS shows four points, marked by black dots, where the function attains a minimum value of zero. These resemble small indentations in the broad brim of a hat. The points of the NW–SE axis differ only by a change of sign. Likewise, the points in the NE–SW axis. The latter fulfil the miniphase or invertibility condition.

The contour map shows a remarkable flatness in the vicinity of the minimising points. This implies that a wide spectrum of the LSE parameter values will give rise to almost identical autocovariance functions and spectra.

The RHS of the diagram provides more evidence of the criterion function in the vicinity of the minima. It shows the contours of the function $q = 1/(z + d)$, where d is a small positive number that prevents a division by zero. We set $d = (X - RM)/(R - 1)$, where $M = \min(z)$, $X = \max(z)$ and where $R = \max(q)/\min(q) = 60$.

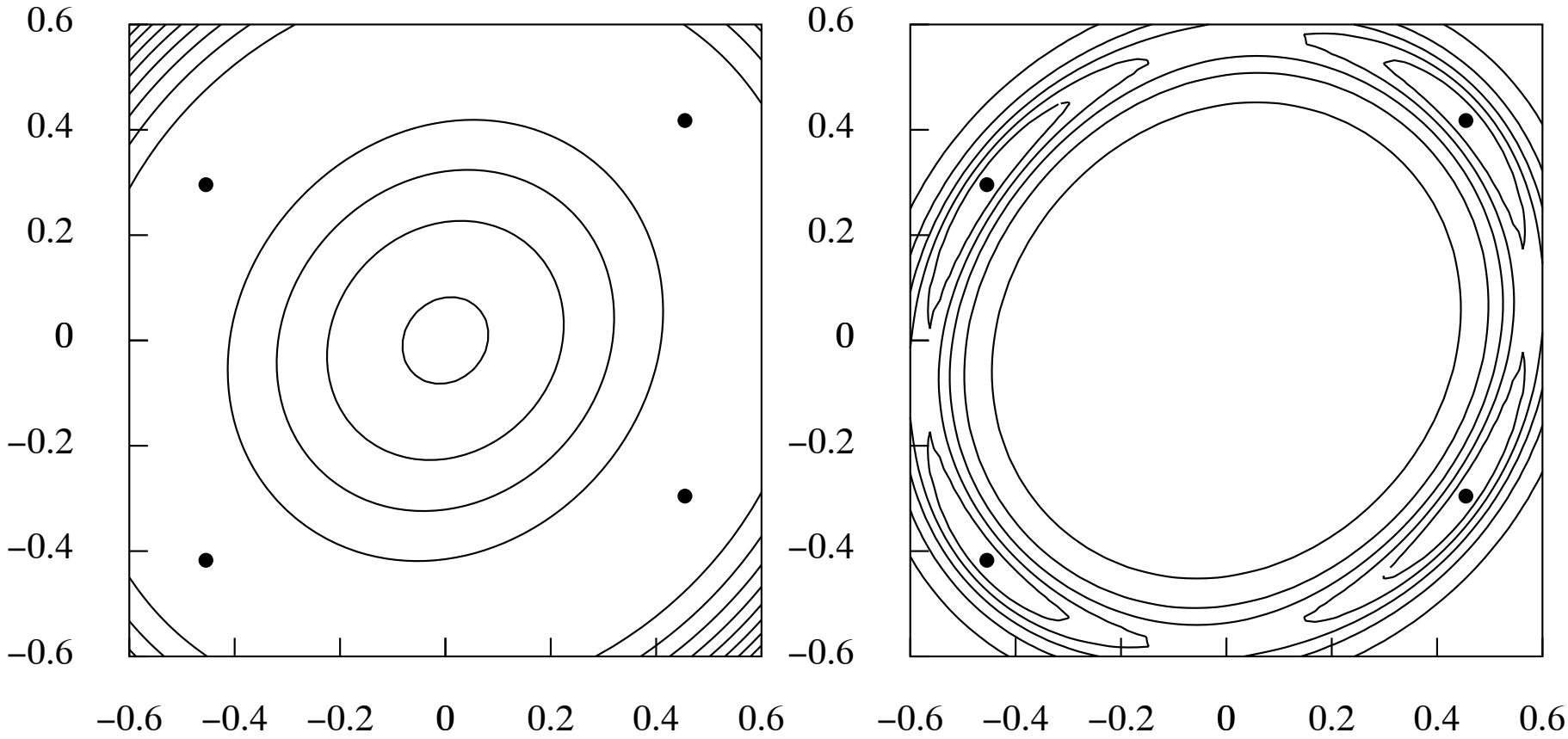

Figure 12. *Left* The contours of the criterion function $z = z(a, b)$ together with the minimising values, marked by black dots. *Right* The contours of the function $q = 1/(z + d)$.

Mapping from an ARMA to an LSDE Model in the Presence of Aliasing

We choose an ARMA model with conjugate complex poles with an argument $\theta = \pi/4 = 45°$, as before, but with a modulus of $\rho = 0.5$. The moving-average component has a zero of 0.5. The ARMA parameters and those of the corresponding LSDE are as follows:

ARMA	LSDE
$\alpha_0 = 1.0$	$\phi_0 = 1.0$
$\alpha_1 = -0.7071$	$\phi_1 = 1.3863$
$\alpha_2 = 0.2500$	$\phi_2 = 1.0973$
$\beta_0 = 1.0$	$\theta_0 = 1.5012$
$\beta_1 = -0.5$	$\theta_1 = 0.8905$

The spectral density functions of the LSDE and of the ARMA model are superimposed on same diagram. The spectrum of the LSDE extends far beyond the Nyquist frequency of π, which is the limiting ARMA frequency.

The ARMA process, which is to be regarded as a sampled version of the LSDE, is seen to suffer from a high degree of aliasing, whereby the spectral power of the LSDE that lies beyond the Nyquist frequency is mapped into the Nyquist interval $[-\pi, \pi]$, with the effect that the profile of the ARMA spectrum is raised considerably.

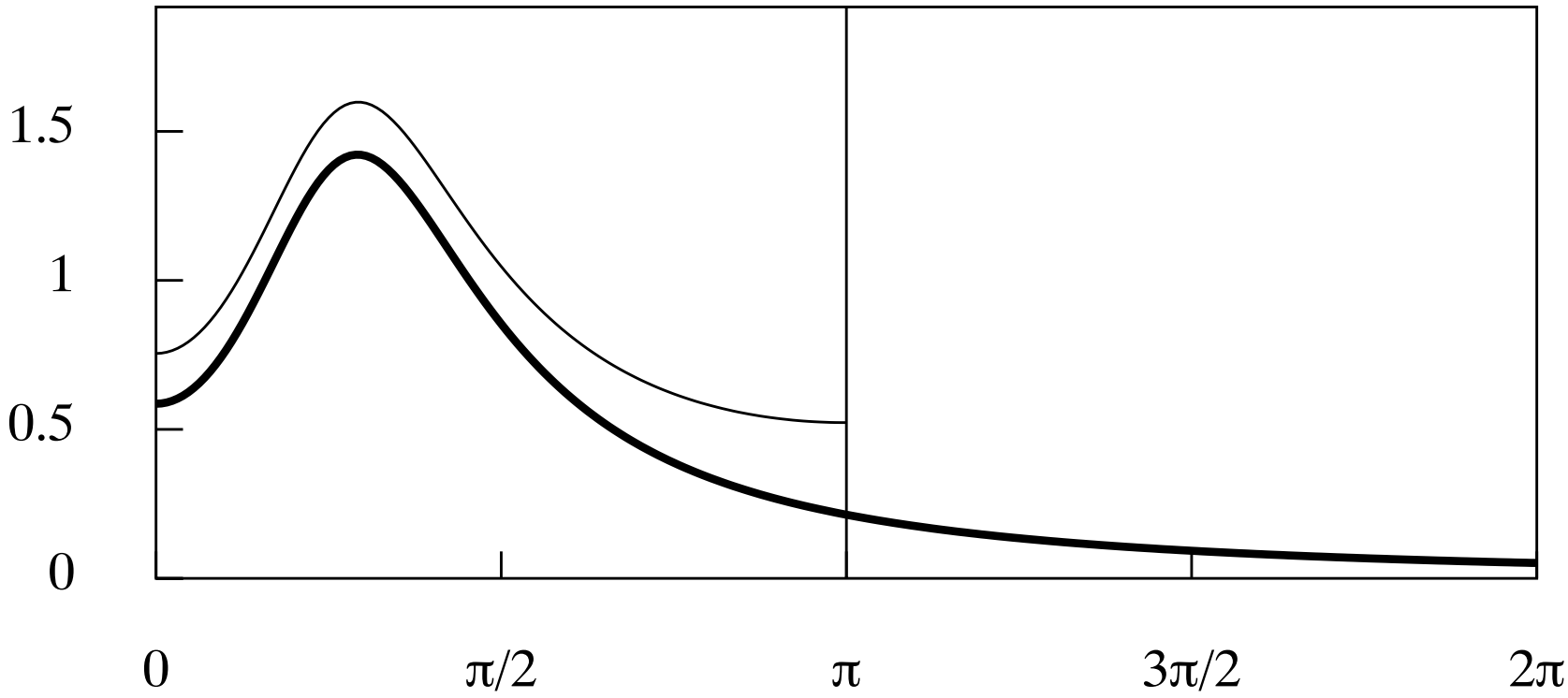

Figure 13. The spectrum of the revised ARMA model superimposed on the spectrum of the derived LSDE, described by the heavier line.

Summary and Conclusions

It will always be possible to find a frequency-limited CARMA model that corresponds to a discrete-time ARMA model, but it is appropriate to do so only if the underlying process is bounded in frequency by the Nyquist value.

If the maximum frequency of the process is less than the Nyquist value, then the process should be resampled at a lower rate to ensure that the maximum frequency corresponds to π radians per sampling interval.

To achieve this, it may be necessary to reconstitute the continuous trajectory of the process from the available sample via a Fourier synthesis.

There are ARMA models for which there are no corresponding LSDE's. Our procedure for translating from an ARMA model to an LSDE reveals such cases by its failure to find a zero-valued minimium of the criterion function. However, it can be relied upon to find the LSDE most closely related to the ARMA model.

The methods for translating from a discrete-time ARMA model to a continuous-time model, which is either a CARMA model of an LSDE, and for translating from such a model back to an ARMA model, have been realised in the computer program CONCRETE.PAS, which is available on the author's website:

`http://www.le.ac.uk/users/dsgp1/`